

# Long-term variations in the north-south asymmetry of solar activity and solar cycle prediction, III: prediction for the amplitude of solar cycle 25

J. Javaraiah

*Indian Institute of Astrophysics, Bengaluru - 560034, India*  
*Tel: +91 80 25530672, Fax: +91 80 25534043*

---

## Abstract

The combined Greenwich and Solar Optical Observing Network (SOON) sunspot group data during 1874–2013 are analysed and studied the relatively long-term variations in the annual sums of the areas of sunspot groups in  $0^\circ - 10^\circ$ ,  $10^\circ - 20^\circ$ , and  $20^\circ - 30^\circ$  latitude intervals of the Sun's northern and southern hemispheres. The variations in the corresponding north-south differences are also studied. Long periodicities in these parameters are determined from the fast Fourier transform (FFT), maximum entropy method (MEM), and Morlet wavelet analysis. It is found that in the difference between the sums of the areas of the sunspot groups in  $0^\circ - 10^\circ$  latitude intervals of northern and southern hemispheres, there exist  $\approx 9$ -year periodicity during the high activity period 1940–1980 and  $\approx 12$ -year periodicity during the low activity period 1890–1939. It is also found that there exists a high correlation (85% from 128 data points) between the sum of the areas of the sunspot groups in  $0^\circ - 10^\circ$  latitude interval of the southern hemisphere during a  $Q$ th year (middle year of 3-year smoothed time series) and the annual mean International Sunspot Number ( $R_Z$ ) of  $(Q + 9)$ th year. Implication of these results is discussed in the context of solar activity prediction and predicted  $50 \pm 10$  for the amplitude of solar cycle 25, which is about 31% lower than the amplitude of cycle 24.

*Keywords:* solar magnetic field, solar activity, solar cycle

---

---

*Email address:* [jj@iiap.res.in](mailto:jj@iiap.res.in) (J. Javaraiah)

## 1. Introduction

Solar activity varies on many timescales (from decades to stellar evolutionary timescales, Rozelot, 2001; Hathaway, 2010; Ahluwalia & Ygbuhay, 2012). Fig. 1 shows the long-term variations in the annual mean monthly Zürich or International Sunspot Number ( $R_Z$ ) taken from the website, <ftp://ftp.ngdc.noaa.gov/STP/space-weather/solar-indices/sunspot-numbers>. The study of variations in the solar activity is important for understanding the basic mechanism of solar cycle and for predicting the level of solar activity.

It is well believed that interactions of solar convection, magnetic field, rotational and meridional flows responsible for solar activity and solar cycle. It is known that solar activity, rotation rate, and meridional velocity are latitude and time dependent. Studies on latitude and time dependent variations of these phenomena are important for understanding the mechanism behind solar cycle, which is not yet fully understood. The latitude and time dependencies in these large-scale flows may cause the magnetic fields at different heliographic latitudes during different time-intervals of a solar cycle for contributing (/relating) the activity at the same or different heliographic latitudes during its following cycle(s). These different latitude bands of activity could produce correlations useful in predictions. Recently, by using the sunspot group data during the period 1874–2006, we have found the following results (Javaraiah, 2007, 2008, hereafter Paper I, Paper II).

1. REL1—The sum of the areas of the sunspot groups in  $0^\circ - 10^\circ$  latitude interval of the Sun's northern hemisphere and in the time-interval of  $-1.35$  year to  $+2.15$  year from the time of the preceding minimum of a solar cycle  $n$  correlate well (correlation coefficient  $r = 0.947$ ) with the amplitude (largest 13-month running smoothed sunspot number) of the next cycle  $n + 1$ . The correlation between the north-south difference of the corresponding area sums in these latitude and time intervals and the amplitude of cycle  $n + 1$  is found to be even much higher ( $r = 0.968$ ).
2. REL2—The sum of the areas of the sunspot groups in  $0^\circ - 10^\circ$  latitude interval of the southern hemisphere and in the time-interval of 1.0 year to 1.75 year just after the time of the maximum of the cycle  $n$  correlate very well ( $r = 0.966$ ) with the amplitude of cycle  $n + 1$ .

The following are the abbreviations and their corresponding meanings that were used in Papers I and II, which are also used (or mentioned) in the present paper.

- $n$  - the Waldmeier solar cycle number,
- $T_m$  - the preceding minimum epoch of a solar cycle,
- $T_M$  - the maximum epoch of a solar cycle,
- $R_m$  - the value of 13-month smoothed  $R_Z$  at  $T_m$ ,
- $R_M$  - the value of 13-month smoothed  $R_Z$  at  $T_M$ ,
- $T_m^*$  - the time-interval of  $-1.35$  year to  $+2.15$  year from  $T_m$ ,
- $T_M^*$  - the time-interval of  $1.0$  year to  $1.75$  year just after  $T_M$ ,
- $A_{N,n}(T_m^*)$  - the sum of the areas of the sunspot groups in  $0^\circ - 10^\circ$  latitude interval of the northern hemisphere during  $T_m^*$  of a cycle  $n$ ,
- $A_{S,n}(T_m^*)$  - the sum of the areas of the sunspot groups in  $0^\circ - 10^\circ$  latitude interval of the southern hemisphere during  $T_m^*$  of a cycle  $n$ ,
- $A_{N,n}(T_M^*)$  - the sum of the areas of the sunspot groups in  $0^\circ - 10^\circ$  latitude interval of the northern hemisphere during  $T_M^*$  of a cycle  $n$ ,
- $A_{S,n}(T_M^*)$  - the sum of the areas of the sunspot groups in  $0^\circ - 10^\circ$  latitude interval of the southern hemisphere during  $T_M^*$  of a cycle  $n$ ,
- $\delta A_n(T_m^*)$  - the difference,  $A_{N,n}(T_m^*) - A_{S,n}(T_m^*)$ , and
- $\delta A_n(T_M^*)$  - the difference,  $A_{N,n}(T_M^*) - A_{S,n}(T_M^*)$ .

The following equations correspond to REL1, obtained in Papers I and II (there are minor/negligible changes in the values of coefficients due to some minor data corrections):

$$R_{M,n+1} = (1.7 \pm 0.2)A_{N,n}(T_m^*) + (74 \pm 7), \quad (1)$$

and

$$R_{M,n+1} = (1.6 \pm 0.1)\delta A_n(T_m^*) + (100 \pm 4). \quad (2)$$

The following equation correspond to REL2, obtained in Paper I:

$$R_{M,n+1} = (1.5 \pm 0.1)A_{S,n}(T_M^*) + (22 \pm 10). \quad (3)$$

It should be noted that the difference in the temporal dependence in the correlations between the sums of the areas of the sunspot groups in the latitude intervals of the northern and southern hemispheres is due to (or it implies) the temporal dependence in the north-south (N-S) asymmetry of the sunspot activity (for details on the N-S asymmetry of solar activity see Javaraiah and Gokhale, 1997; Chang, 2009, Papers I and II, and references therein). Although both the relations REL1 and REL2 are based on almost equal high correlations, they yielded a substantial different values for the amplitude of solar cycle 24, *viz.*  $103 \pm 10$  and  $74 \pm 10$ , respectively. The current trend (not shown in Fig. 1) of 13-month smoothed monthly  $R_Z$  indicates two peaks (Gnevyshev peaks) for the current solar cycle 24: one with value 66.9 in February, 2012 and another with value 75 in October, 2013. Obviously the prediction based on the REL1 seems to be failed. The value  $74 \pm 10$  predicted from the REL2, i.e., by using Equation (3), within its uncertainty limits is close to the observed  $R_M$ .

In the present analysis we determined the long-term periodicities in the differences (N-S asymmetries) between the sums of the areas of the sunspot groups in different  $10^\circ$  latitude intervals of the northern and southern hemispheres by using FFT and MEM. The time-dependencies in the periodicities are checked by using the Morlet-wavelet analysis. We checked whether REL1 and REL2 are connected to long-term periodicities in the N-S asymmetry of sunspot activity. By using REL2 it is possible to predict only the amplitude of a cycle with a good accuracy by about 9-year advance. Therefore, here we have also checked whether it is possible to predict the annual mean  $R_Z$ , by determining the cross-correlations between the annual mean  $R_Z$  and the annual sum of the areas of sunspot groups in different  $10^\circ$  latitude intervals. That is, we checked whether it is possible to predict the shape and length of a solar cycle, and also the epoch and the strength its minimum. In addition, by using REL1 and REL2 (mainly), we predicted the amplitude of solar cycle 25.

It should be noted here that, for the first time in the solar cycles history, in the case of solar cycle 24 the second peak is larger than the first peak. REL2 seems to be related to the Gnevyshev gaps as well as the epoch of change in the sign of global magnetic field. In the current cycle the polarities of north-pole magnetic fields are already changed. Therefore, although the epoch of maximum of cycle 24 may be October 2013, we have made a tentative prediction for the amplitude of cycle 25 by using REL2 with reference to the first peak at February 2012.

In the next section we will describe data and method of analysis. In Section 3 we will present results, and in Section 4 we will present conclusions and a brief discussion.

## 2. Data and method of analysis

In Papers I and II we have used the Greenwich sunspot group data during 1874–1976 and the SOON sunspot group data during 1977–2006. Now SOON sunspot group data are used for seven more years, 2007–2013 (the data are available up to date) and are also taken from the David Hathaway’s website <http://solarscience.msfc.nasa.gov/greenwich.shtml>. The data analysis is carried out by taking all the precautions that were taken in Papers I and II. We determined the annual variations in the sums of the areas of sunspot groups in different  $10^\circ$  latitude intervals. The calculations were done for each year data separately and also by binning the data into 3-year moving time intervals (3-year MTIs) successively shifted by one year during the period 1874–2013, for the sake of better statistics. The time series of the sums of the areas of sunspot groups in different  $10^\circ$  latitude intervals are cross-correlated with the annual time series of  $R_Z$ .

The long-term periodicities in the north-south differences (N-S asymmetries) of the sums of the areas of sunspot groups in different  $10^\circ$  latitude intervals are determined from the FFT analysis, the values of the periodicities are determined by using MEM, and the Morlet wavelet analysis is used to find the temporal dependence in the periodicities. In the case of long and evenly spaced time series (windows), Fourier transform method is a powerful tool, whereas in the case of short time series the Fourier components can only be determined at harmonics of the fundamental frequency. Besides FFT we have used here MEM because it is a powerful spectral method for detecting the relevant longer periodicities from a short time series (a brief description about the MEM and the wavelet analysis is given below, also see Javaraiah, 2011).

Essentially MEM involves fitting an autoregressive model to the data based on the principle that the resultant spectral estimate should be based on all the information in the actual record and assume the least possible amount of information (hence the name maximum entropy) about the series outside the observed record. The condition for this happens to be satisfied by the  $\mu$ th order autoregressive process. An important step in this method is the optimum selection of  $\mu$ , which is the number of immediately previous

points that have been used in the calculation of a new point. If  $\mu$  is chosen too low the spectrum is over-smoothed and the high resolution potential is lost. If  $\mu$  is chosen too high, frequency shifting and spontaneous splitting of the spectral peaks occurs, giving a false peaky appearance to the spectrum. Objective methods for selecting  $\mu$  have been suggested by a number of authors (see Barton, 1983). The MEM code which we have used here takes the values for  $\mu$  in the range  $(\tau/3, \tau/2)$  (Ulrych and Bishop, 1975) or  $2\tau/\ln(2\tau)$  (Berryman, 1978), where  $\tau$  is the size of a time series. We have computed MEM power spectra choosing various values for  $\mu$  in the range  $(\tau/3, \tau/2)$  and  $2\tau/\ln(2\tau)$ . We find that  $\mu = \tau/3$  is suitable in the present MEM analysis, *i.e.*, in the derived spectra the peaks are considerably sharp and separated.

Wavelet analysis helps to find simultaneously the periodicities in a time series and the temporal dependence in the corresponding amplitudes of the periodicities. We have used the wavelet IDL code provided by Ch. Torrence and G. P. Compo as described in Torrence and Compo (1998). A wavelet is a function with zero mean and that is localised in both frequency and time. The Morlet wavelet is defined as

$$\psi_0(\eta) = \pi^{-\frac{1}{4}} e^{i\omega_0\eta} e^{-i\frac{1}{2}\eta^2} ,$$

where  $\omega_0$  is dimensionless frequency and  $\eta$  is dimensionless time. The Morlet wavelet (with  $\omega_0 = 6$ ) is a good choice, because it provides a good balance between time and frequency space (Grinsted *et al.*, 2004). The wavelet is stretched in time by varying its scale ( $s$ ) and normalising it to have unit energy. Thus,  $\eta = s.t$ , where  $t$  is time. The wavelet scale  $s$  is almost identical to the corresponding Fourier period, *i.e.*, the Morlet wavelet with  $\omega_0 = 6$  gives  $\lambda = 1.03s$ , where  $\lambda$  is the Fourier period. Regions where edge effects become important, because of the finite length of the time series, are labelled as cone of influence (COI). The time series is padded with sufficient zeroes to bring the total length of the time series up to the next power of two, limiting the edge effects and speeding up the Fourier transform (for more details see Torrence and Compo, 1998)).

### 3. Results

Fig. 2 shows the variations in the annual sums of the areas of the sunspot groups,  $A_N(t)$  and  $A_S(t)$ , in  $0^\circ - 10^\circ$  latitude intervals of the northern and southern hemispheres during the period 1875–2013. In the same figure the

variations in  $A_N(T_m^*)$ ,  $A_S(T_M^*)$ , and the annual mean of  $R_Z$  are also shown. Fig. 3 is the same as Fig. 2 but the variations in  $A_N(t)$  and  $A_S(t)$  are determined by binning the sunspot group data during the period of 1875–2013 into 3-year MTIs. In this case  $t = 1976, 1977, \dots, 2011, 2012$  are the middle years of the 3-year MTIs 1875–1877, 1876–1878,  $\dots$ , 2010–2012, 2011–2013, respectively. In these figures it is easy to identify the locations of  $T_m^*$  and  $T_M^*$ . We use the 3-year MTIs time series because to avoid the gaps in the time series (in Fig. 2 it can be seen that the values of the sums of the areas of sunspot groups are zeros during the minima of some solar cycles). Fig. 4 shows the variations in the north-south difference  $A_N(t) - A_S(t)$ , where  $A_N(t)$  and  $A_S(t)$  are determined from 3-year MTIs (which are shown in Fig. 3). In this figure we have also shown  $\delta A(T_m^*)$  and  $\delta A(T_M^*)$ .

As can be seen in Figs. 2 and 3, the epochs of the maxima and the minima of  $A_N(t)$  and  $A_S(t)$  are not exactly same as those of  $R_Z$ . In fact, there is a suggestion of a few year phase difference between each of these quantities and  $R_Z$ . The phase difference is determined below. As can be seen in Fig. 4, the N-S asymmetry, i.e.  $A_N(t) - A_S(t)$  is considerably vary and there is a suggestion for the existence of a few long-term periodicities in it.

Fig. 5 shows the FFT power spectra of the N-S asymmetry (N-S difference) in the sums of the areas of the sunspot groups in each different  $10^\circ$  latitude intervals. The corresponding MEM and wavelet spectra are shown in Figs. 6 and 7, respectively. As can be seen in Fig. 5, in the FFT power spectrum that correspond to  $0^\circ - 10^\circ$  latitude interval, the peak at the corresponding frequency of  $\approx 8.5$ -year periodicity is significant on slightly above 99% confidence level ( $2.8\sigma$ ). The corresponding peak is highly insignificant in the FFT power spectrum that correspond to  $20^\circ - 30^\circ$  latitude interval. There is a relatively less significant ( $1.85\sigma$ ) peak at the corresponding frequency of 9.7-year periodicity in the FFT power spectrum that correspond to  $10^\circ - 20^\circ$  latitude interval. In this spectrum there is also a peak at the corresponding frequency of  $\approx 15.1$ -year periodicity, which is significant on 98% confidence level. In the corresponding FFT spectra of the  $0^\circ - 10^\circ$  and  $10^\circ - 20^\circ$  latitude intervals there are peaks at frequency correspond to the  $\approx 12.4$ -year periodicity, which are significant on slightly larger than 96% confidence level ( $2.1\sigma - 2.5\sigma$ ). All the three spectrum show peaks at the corresponding frequency of 60–100 year periodicity. The peak at this frequency is relatively weak (statistically insignificant) in the case of the spectrum that correspond to  $0^\circ - 10^\circ$  latitude interval. The corresponding MEM spectra indicate the values of all these periodicities as 66.7-year, 16-year, 12.5-year, and 8.7-year. There are other

relatively short periodicities (7-year, 5.5-year and 4-year), but they can be seen mainly in the MEM spectrum that correspond to  $20^\circ - 30^\circ$  latitude interval. Overall the known  $\approx 9$  year periodicity in the N-S asymmetry of the sunspot area (Chang, 2009) exists mainly in below  $20^\circ$  latitudes (it is very weak in  $20^\circ - 30^\circ$  latitude interval). The  $\approx 12.5$ -year periodicity, which is found in N-S asymmetry of sunspot activity (Carbonell *et al.*, 1993; Javaraiah and Gokhale, 1997), is much clear in the MEM spectrum that correspond to  $0^\circ - 10^\circ$  latitude interval. The 44–55 year cycles can be seen in both  $\delta A(t_m^*)$  and  $\delta A(T_M^*)$  (see Fig. 4).

As can be seen in Fig. 7, the  $\approx 9$ -year periodicity exists in all the three latitude intervals, but it was mainly exist during the high activity period 1940–1980. The  $\approx 12.5$ -year periodicity exists in  $0^\circ - 10^\circ$  latitude interval mainly during the low activity period 1890–1939. The temporal dependence of the  $\approx 12.5$ -year periodicity is not clear in the other two latitude intervals. In the wavelet spectra the  $\approx 60$ -year periodicity is not well defined, i.e. it is within the cross-hatched region throughout the period 1875–2013. Of course, this periodicity is obviously connected to the two components of the last Gleissberg cycle: the high activity 9-year periodicity and the low activity 12-year periodicity portions of the north-south difference in the sunspot activity at  $0^\circ - 10^\circ$  latitude interval. This may indicate that the current period could be low activity portion of the ongoing Gleissberg cycle.

[In the FFT and MEM spectra (not shown here) of the sums of the areas of the sunspot groups in the individual latitude intervals of northern and southern hemispheres, the 11-year periodicity is found dominant in all the three latitude intervals of each hemisphere. A 8–9 year periodicity is also seen in the MEM spectra of all the latitude intervals of southern hemisphere, and is not seen in the spectrum that correspond to any of the three latitude intervals of northern hemisphere. In the wavelet spectra (not shown) that correspond to the individual intervals of the northern and southern hemispheres, the 9-year and 12-year periodicities are found to be unresolved.]

We calculated the cross-correlations between  $A_N(t)$  and annual  $R_Z(t)$ , and also between  $A_S(t)$  and annual  $R_Z(t)$  (in the case of  $R_Z(t)$ ,  $t$  represents actual year). For this purpose also the time series of 3-year MTIs are used. We determined the cross-correlations, besides in  $\pm 0^\circ - 10^\circ$  latitude interval, in  $\pm 10^\circ - 20^\circ$  and  $\pm 20^\circ - 30^\circ$  latitude intervals also. The cross correlations are shown in Fig. 8. As can be seen in this figure, the cross-correlation coefficient (*CCF*) varies systematically (damped wave like behaviour) with *Lag* (absolute), implying that the area-sums vary systematically similar to



$R_Z$ . In the case of  $0^\circ - 10^\circ$  latitude interval, the peak of  $CCF(R_Z, A_S)$  at  $Lag = -9$  is large (with value 0.79) and statically high significant as that of the one close to  $Lag = +1$  (with value 0.83). The peak of  $CCF(R_Z, A_N)$  is much smaller (0.66) at  $Lag = -9$ , and slightly larger (0.83) at  $Lag = +1$ , than the corresponding peaks of  $CCF(R_Z, A_S)$ . In the cases of  $10^\circ - 20^\circ$  and  $20^\circ - 30^\circ$  latitude intervals,  $CCF(R_Z, A_S)$  and  $CCF(R_Z, A_N)$  have dominant peaks at  $Lag = 0$  and  $Lag = -1$ , receptively and the peaks at  $Lag = -9$  are considerably smaller than the corresponding one of  $CCF(R_Z, A_S)$  in  $0^\circ - 10^\circ$  latitude interval. The differences between the peaks of  $CCF(R_Z, A_N)$  and  $CCF(R_Z, A_S)$  are larger in the case of  $0^\circ - 10^\circ$  latitude intervals than corresponding differences in the other two latitude intervals, particularly for negative values of  $Lag$ .

A peak of  $CCF$  at a negative value of  $Lag$  implies that the corresponding  $A_N$  or  $A_S$  leads  $R_Z$ . That is, in the case of  $CCF(R_Z, A_S)$  of  $0^\circ - 10^\circ$  latitude interval the presence of a dominant peak at  $Lag = -9$  implies  $A_S$  leads  $R_Z$  by about nine years. This is consistent with the high correlation between  $A_{S,n}(T_M^*)$  and  $R_{M,n+1}$  (*cf.* REL2).

Fig. 9 shows the scatter plot of  $A_S(t)$  of the sunspot groups in  $0^\circ - 10^\circ$  latitude interval of the southern hemisphere versus  $R_Z(t+9)$ . In this figure the continuous curve represents the following linear relationship between  $A_S(t)$  and  $R_Z(t+9)$ :

$$R_Z(t+9) = (0.47 \pm 0.03)A_S(t) + (11 \pm 3). \quad (4)$$

The corresponding values of the correlation coefficient ( $r = 0.85$ ) and the slope are statistically high significant (derived from 128 data points, from the Student's t-test  $P < 0.01$ ).

Fig. 10 shows the plots of the simulated (by using Equation (4)) and the observed values of the yearly mean  $R_Z$  versus time (year). In this figure it can be seen that the shape of the simulated cycle 24 is almost same as the pattern of temporal behaviour of  $A_S(t)$  of the sunspot groups in  $0^\circ - 10^\circ$  latitude interval of the southern hemisphere during cycle 23 (see Fig. 3). The simulated value  $120 \pm 24$  for  $R_M$  of cycle 24 is almost equal to the observed as well as the simulated values of  $R_M$  of cycle 23, a contradiction to all the corresponding predictions for  $R_M$  of cycle 24 in Papers I and II. The simulated amplitudes of some small/large cycles are considerably larger/smaller than the corresponding observed amplitudes, causing the uncertainty of the simulated value is high ( $\sigma = 24$ ), making the reliability of this simulated  $R_M$

of cycle 24 is lower than the previous predictions that were made by using REL2 (or even that was made by using REL1). As per the current level of sunspot activity it seems to be almost certain that the simulated value is much higher than the real observed amplitude of cycle 24. In fact, in Paper II we have noticed that a higher value of predicted  $R_M$  correspond to a lower value of  $r$ . The lengths of solar cycles considerably vary. In addition, the wavelet analysis suggests that the long-term periodicities in  $A_S(t)$  are time dependent. Consequently, for prediction purpose it is not possible to use directly the continuous time series of  $A_S(t)$  in equal time intervals. That is, it is necessary to take the variations in the lengths of solar cycle into account. It should be noted here that even in the case of the prediction of  $R_M$  of a cycle by using the polar fields at minimum of the cycle could more uncertain and fail if the polar fields were used early before the start of the cycle (Svalgaard *et al.*, 2005). That is, in our method also it is necessary to find the exact epoch in which the sum of the areas of the sunspot groups highly correlated with  $R_M$  of next cycle. For the same reason we have used the method described in Papers I and II and found REL1 and REL2.

In Fig. 10 there is an indication that 2011 is the epoch of maximum of cycle 24. There is a suggestion that this cycle also may be somewhat long and the next minimum may be also weak similar to the last (between cycles 23 and 24) very weak minimum. There is also a suggestion that a secondary peak will occur in the year 2014. The rise to maximum may be also steep in cycle 24 as that of cycle 23. Interestingly, within the year 2011 a very large peak exists in the monthly variation in  $R_Z$  (the corresponding figure is not shown here). Some recent analysis suggested that in the northern hemisphere the maximum is already occurred in the year 2011, but not in the southern hemisphere (Gopalswamy *et al.*, 2012). Since we have correlated the 3-year MTI's sum of the areas of sunspot groups with the annual mean  $R_Z$  (mean of the monthly mean values of  $R_Z$ ), one can expect the uncertainties up to 12 months in the simulated epochs of maxima and minima. However, overall we can draw a conclusion that the Eq. (4) is not much useful for prediction purpose. (There is a considerable spread in Fig. 9. The error in the sum of the areas of sunspot groups is an essential part of the present analysis, but that error is difficult to generate here because the values of the errors in the areas of sunspot groups are not available/known.)

REL2 is essentially a special case of the  $A_S(t) - R_Z$  relationship (cf., conclusion 2 and Eq. (4)) correspond to the peak of  $CCF$  at  $Lag = -9$  year. The peak of  $CCF$  at  $Lag = 1$  to 2 years suggest the existence of a relation

between  $R_M$  and  $A_S(T_M^*)$  of a cycle, but we find a very weak correlation ( $r = 0.34$ ) between these parameters of a cycle. That is,  $R_Z$  of a year may have an effect on  $A_S$  of the following year, but may not be beyond one year. Therefore, it seems  $R_M$  of cycle does not have a strong affect on  $A_S(T_M^*)$  of the same cycle.  $A_S(T_M^*)$  may represent the proxy of new magnetic flux or largely the magnetic flux that transported from the northern hemisphere do to the equatorial cross of the flux at  $T_M^*$ . It should be noted here,  $T_M^*$  is close to the epoch of global change in the sign of the solar magnetic field. That is, overall it seems REL2 related to the global change in the sign of the solar magnetic field. The  $T_M^*$  of cycle  $n$  and  $T_M^*$  of cycle  $n + 1$  are at the beginning and at about one year before the ending of a half solar magnetic cycle, respectively. It is not clear whether the REL2 related to the approximate 9-year periodicity in the north-south difference of the sum of the areas of sunspot groups in the  $0^\circ - 10^\circ$  latitude intervals of the northern and southern hemispheres, because the wavelet analyses suggest that the approximate 9-year periodicity does not exist continuously throughout 1875–2013.

#### 4. Prediction for the amplitude of solar cycle 25

As already mentioned in section 1, although the values of of the corresponding correlation coefficients of both the relations REL1 and REL2 are almost equal and high, they yielded a substantial different values for the amplitude of solar cycle 24, *viz.*  $100 \pm 10$  and  $74 \pm 10$ , respectively. A plausible reason for this could be due to the missing of some normalisation factor between these relationships. On the other hand, the REL2 is better defined than that of REL1, in the sense that the intercepts of the corresponding linear equations have a small ( $22 \pm 10$ ) and a large ( $74 \pm 10$ ) values, respectively. That is, one-to-one correspondence between  $R_M$  and  $A_S(T_M^*)$  is much stronger than that between  $R_M$  and  $A_N(T_m^*)$ . Observationally, the uncertainty in  $A_N(T_m^*)$  is more than that in  $A_S(T_M^*)$  because the data near the maximum of a solar cycle is well measured(/defined) than that at the minimum. By solving Eq. (1) that correspond to REL1 and Eq. (3) that correspond to REL2, we get a new equation which is free of constant term. From this way in Paper-I it was obtained  $57 \pm 13$  for  $R_M$  of cycle 24. Similarly, if we solve Eqs. (2) and (3), we get

$$R_{M,n+1} \approx 1.98 \times A_{S,n}(T_M^*) - 0.46 \times \delta A_n(T_m^*). \quad (5)$$

By using Eq. (5) we get  $66 \pm 13$  for  $R_M$  of cycle 24 which is almost equal to the value of the first peak of cycle 24. As per the current level of sunspot activity, it is almost certain that this, and the value  $74 \pm 10$  that was predicted by using REL2 alone, will be very close to the reality.

The value of about 100 found from REL1 for amplitude of cycle 24 seems to be certainly failed. However, by using REL1 it seems still possible to make a prediction qualitatively (*i.e.*, it seems to be possible to find whether the next cycle is stronger or weaker than the immediate previous one) by 13-year advance (that was the major conclusion about the values that were obtained by using REL1 in Papers I and II). For this, one can also utilise the following relationship:  $A_{S,n}(T_M^*) \approx 1.5A_{N,n}(T_m^*) + 50$ . That is, first obtain the approximate value of  $A_{S,n}(T_M^*)$  by using this relationship and then by substituting that in Eq. (3). (In Paper II some other simple additions of the values of the parameters of REL1 and REL2 were carried out and obtained few other values, obviously they are incorrect though each one of them is less than the amplitude of cycle 23. Even these earlier predictions indicated that certainly cycle 24 will be weaker than cycle 23).

The maximum (in  $R_Z$ ) of a solar cycle is not smooth. Two or more peaks can be identified during the solar maxima and are called Gnevyshev peaks, because this splitting of activity was identified for the first time by Gnevyshev (1967, 1977). The time interval between these peaks, where the level of activity is relatively low, is known as the Gnevyshev gap (see the review by Storini, 2003). Incidentally, the epochs of  $T_M^*$  seem to be close to the Gnevyshev gaps and also close to the time when the sign of the magnetic field is changing in the northern and southern hemispheres. At these occasions there could be interactions of the plasma flows of opposite polarities causing cancellation of magnetic flux. (At these occasions of a cycle downward flow may also taking place, which may provide required resource for next cycle.) Overall, it seems REL2 related to the global change in the sign of the solar magnetic field. In fact, the  $T_M^*$  of cycle  $n$  and  $T_M$  of cycle  $n + 1$  are at the beginning and near the ending of a same half solar magnetic cycle, respectively. Georgieva and Kirov (2011) suggested that the double peaks and the Gnevyshev gap in sunspot maximum can be explained as the sunspot maximum is the superposition of the two surges of toroidal magnetic field generated by two parts of the poloidal field. One part generated at the surface is advected by the meridional circulation all the way to the poles and another part is diffused directly to the tachocline at mid-latitudes. One can also think that the cause of the Gnevyshev peaks/gaps may be due to interaction of at least

two magnetic waves whose amplitudes and phases are different. Therefore, Eq. (5), which is the linear combination of Eqs. (2) and (3), may be having the aforementioned physical background rather than mere mathematical.

Here we have used SOON sunspot data for seven more years and found that the latest  $T_m^*$  and  $T_M^*$  (with reference to the first peak of  $R_Z$  at 2012.170) are 2007.55 – 2011.05 and 2013.17 – 2013.92, and the values of the corresponding  $A_N(T_m^*)$  and  $A_S(T_M^*)$  are 0.48 and 18.86, respectively.

In principle, according to REL1, *i.e.* by using Eqs. (1) and (2), it should be possible to make a prediction for  $R_M$  of solar cycle 25. By using Eq. (2) we obtained  $84 \pm 10$  for  $R_M$  of cycle 25, which is much lower than the corresponding predicted value ( $100 \pm 10$ ) for  $R_M$  of cycle 24, but  $R_M \approx 75$  of cycle 24 is much less than 84. Therefore, this result only indicates that the cycle 25 could be relatively weaker (not represents the amplitude of cycle 24), suggesting that the REL1 (Eqs. (1) and (2)) can be used to make a qualitative prediction for the amplitude of a cycle. That is, Eqs. (1) and (2) can be used to know whether the amplitude of next cycle is less or greater than that of previous one, by about 13 year advance.

On the other hand by using REL2, *i.e.* by using Eq. (3), we can make a reasonably accurate prediction. By using using Eq. (3) we get  $50 \pm 10$  for  $R_M$  of cycle 25. By using Eq. (5) we get  $42 \pm 13$  (Note: in this case the latest value of  $\delta A_n(T_m^*) = -9.77$ ).

We would like to make the following clarifications about our methods of analysis: Fig. 11 shows the changes in the correlations as the changes in  $T_m^*$  and  $T_M^*$ . Here we have used 1.0 year (instead of 0.05 year used in Papers I and II) increase/decrease in each successive iteration. The end points of the time intervals (represented by the interval numbers) are away from  $T_m$  and  $T_M$  as follows: Intervals 1, 2, 3, 4, ..., 7 are at (-2, -1) (-2, 0), (-2, 1), (-2, 2), ..., (-2, 5) years away, respectively; the end points of the intervals 8, 9, ..., 13 are at (-1, 0) (-1, 1), ..., (-1, 5) years away, respectively; similarly, the end points of the intervals 19, 20, ..., 22 are at (1, 2), (1, 3), ..., (1, 5) years away, respectively; and those of the intervals 26 and 27 are at (3, 4) and (3, 5) years away, respectively. In the intervals 4 and 19 the corresponding correlation coefficients have large values, 0.85 and 0.91, respectively. From  $T_m$  and  $T_M$  the end points of the intervals 4 and 19 are at (-2, 2) and (1, 2) years away, respectively, and obviously  $T_m^*$  and  $T_M^*$  are within these intervals, respectively. The increase/decrease time 0.05 year that was used in Papers I and II for accurately determining  $T_m^*$  and  $T_M^*$  may be small, but  $T_m^*$ , and even  $T_M^*$ , are relatively long and the corresponding correlations are still high

with plus or minus of a few times of 0.05 year from these intervals. That is, there is a considerable consistency in the data sampling.

In Fig. 11 (which demonstrates the methodology used in Papers I and II) there are steep changes in the correlation coefficient correspond to the data in  $0^\circ - 10^\circ$  latitude interval of the southern hemisphere, and the variation in the correlation coefficient correspond to the data in  $0^\circ - 10^\circ$  latitude interval of the northern hemisphere is somewhat gradual. In Fig. 2 one can find that the aforementioned steep/gradual changes seen in Fig. 11 is a property of the solar cycle variations in the sum of the areas of the sunspot groups in  $0^\circ - 10^\circ$  latitude interval of the southern/northern hemisphere. That is,  $T_M^*$  is close to the epoch of maximum (peak) of the solar cycle variation in the sum of the areas of the sunspot groups in  $0^\circ - 10^\circ$  latitude interval of the southern hemisphere, where obviously the variation is steep. The  $T_m^*$  is close to the epoch of minimum of the solar cycle variation in the sum of the areas of sunspot groups in  $0^\circ - 10^\circ$  latitude interval of the northern hemisphere, where the variation is somewhat gradual. These results strongly indicate that  $T_m^*$  and  $T_M^*$  are reasonably well defined and hence both the relations REL1 and REL2 are reliable.

## 5. Conclusions and discussion

We analysed the combined Greenwich and SOON sunspot group data during the period 1874–2013 and found the following results:

1. In the difference between the sums of the areas of the sunspot groups in  $0^\circ - 10^\circ$  latitude intervals of northern and southern hemispheres, there exist  $\approx 9$ -year periodicity during the high activity period 1940–1980 and  $\approx 12$ -year periodicity during the low activity period 1890–1939.
2. There exists a high correlation (85% from 128 data points) between the sum of the areas of the sunspot groups in  $0^\circ - 10^\circ$  latitude interval of the southern hemisphere during a  $Q$ th year and ( $R_Z$ ) of  $(Q + 9)$ th year.
3. By using the above relationship (conclusion 2) it is not possible to make an accurate prediction for the amplitude of a solar cycle.
4. Because of the lengths of solar cycles considerably very and the long-term periodicities in  $A_S(t)$  are time dependent (conclusion 1), it is necessary to find the exact epoch in which the sum of the areas of the sunspot groups highly correlated with  $R_M$  of next cycle. Thus, REL2 is a special case of the above relationship (conclusion 2). By using REL2

(Eq. (3)) it is possible for predicting the amplitude of a solar cycle with a good accuracy.

5. We predict  $50 \pm 10$  for the amplitude of the next cycle 25, which is about 31% lower than the amplitude of cycle 24 (in fact, it seems to be lowest compare with the amplitudes of cycles 1–24.).

According to Gnevyshev and Ohl rule (Gnevyshev and Ohl, 1948) or G-O-rule an odd numbered cycle is always stronger than its preceding even numbered cycle. By using the G-O rule it will not be possible to predict the amplitude of solar cycle 25 when the amplitude of solar cycle 24 is known, unless the epochs of the violations of the G-O rule is known in well advance. Using the relations REL1 and REL2 it is possible to predict  $R_M$  of any cycle, *i.e.* an even-numbered solar cycle as well as an odd-numbered solar cycle (no need to know in advance the epochs of violations of the G-O rule). The violation of the G-O rule is followed by a few (at least one) relatively weak solar cycles (see Fig. 1). For example, solar cycle pair (4, 5) was followed by weak solar cycles 6 and 7, solar cycle pair (8, 9) was also followed a relatively weak cycle 10. Thus, one or two weak solar cycles which follow solar cycle pair (22, 23) may be also relatively weak. The low values predicted above for solar cycles 24 and 25 are consistent with this long-term property of solar activity. The predicted amplitudes of cycles 24 and 25 suggest that the G-O rule will be violated by this cycle pair (24, 25) also. That is, it seems for the first time violation of G-O rule takes place in two consecutive pairs of even- and odd-numbered solar cycles, (22, 23) and (24, 25), since G-O rule was discovered.

The long term trend, in fact, extrapolation of the cosine curve shown in Fig. 5 of Javaraiah, Bertello, and Ulrich (2005) from the epoch of cycle 23, suggests that solar cycles 24 and 25 will be relatively weak cycles. The above predicted amplitudes of solar cycles 24 and 25 are consistent with this result. Thus, our predictions are also consistent with the speculation that the minimum of the current Gleissberg cycle will take place in cycle 25 (Javaraiah, Bertello, and Ulrich, 2005). The current long-term minimum (shall include cycles 24 and 25) is at the end of the current Gleissberg cycle (preceding minimum of the next Gleissberg cycle) and it may be similar to the recent Modern Minimum (or even to the Dalton Minimum).

Since our results/predictions are based on the north-south asymmetries in the sums of the areas of the sunspot groups in the heliographic latitudes that are close to the equator, cancellation/enhancement of magnetic flux due to

equatorial crossings of magnetic flux (caused by the solar meridional flows) may have a major role in the mechanism behind our methodology/results.

## Acknowledgments

The author thanks the anonymous referee for useful comments and suggestions. Wavelet software was provided by Ch. Torrence and G.P. Compo, and is available at URL: <http://poas.colorado.edu/research/wavelets/>. The MEM FORTRAN code was provided to us by Dr. A.V. Raveendran.

## References

- Ahluwalia, H.S., Ygbuhay, R.C., 2012. *Adv. Astron.* 2012, Article ID 126516.
- Barton, C., 1983, *Geophys. Sur.* 5, 335.
- Berryman, J.G., 1978. *Geophys.* 43, 1384.
- Carbonell, M., Oliver, R., Ballester, J.L., 1993. *A&A* 274, 497.
- Chang, H-Y., 2009. *NewA* 14, 133.
- Georgieva, K., Kirov, B., 2011. *JASTP* 73, 207.
- Grinsted, A., Moore, J.C., Jevrejeva, S., 2004. *Nonlinear Proc. Geophys.* 11, 561.
- Gnevyshev, M.N., 1967. *SoPh.* 1, 107.
- Gnevyshev, M.N., 1977. *SoPh.* 51, 175
- Gnevyshev, M.N., Ohl, A.I., 1948. *AZ* 25, 18.
- Gopalswamy, N., Yashiro, S., Makela, P., Michalek, G., Shibasaki, K., Hathaway, D.H., 2012. *ApJ* 750, L42.
- Hathaway, D.H., 2010. *Living Reviews in Solar Phys.* 7, 1.
- Javaraiah, J., 2007. (Paper I). *MNRAS* 377, L34.
- Javaraiah, J., 2008. (Paper II). *SoPh.* 252, 419.
- Javaraiah, J., 2011. *SoPh.* 270, 463.



- Javaraiah, J. Gokhale, M.H., 1997. SoPh. 170, 389.
- Javaraiah, J., Bertello, L., Ulrich, R.K., 2005. SoPh. 232, 25.
- Rozelot, J.P., 2001. JASTP 63, 375.
- Storini, M., Bazilevskaya, G.A., Flükiger, E.O., Krainev, M.B., Makhmutov, V.S., Sladkova, A.I., 2003. Adv. Space Res. 31, 895i.
- Svalgaard, L., Cliver, E.W., Kamide, Y., 2005. Geophys. Res. Lett. 32, L0114.
- Torrence, Ch., Compo, G.P., 1998. Bull. Am. Meteor. Soc. 79, 61.
- Ulrych, T.J., Bishop, T.N., 1975. Rev. Geophys. Space Phys. 13, 183.

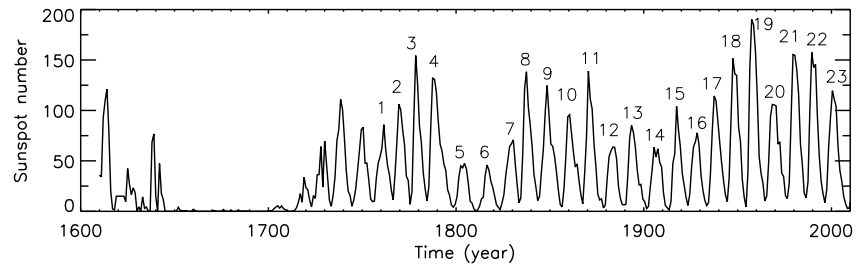


Figure 1: Plots of annual mean international sunspot number ( $R_Z$ ) against time. Near the peaks of the cycles corresponding Waldmeier solar cycle numbers are shown.

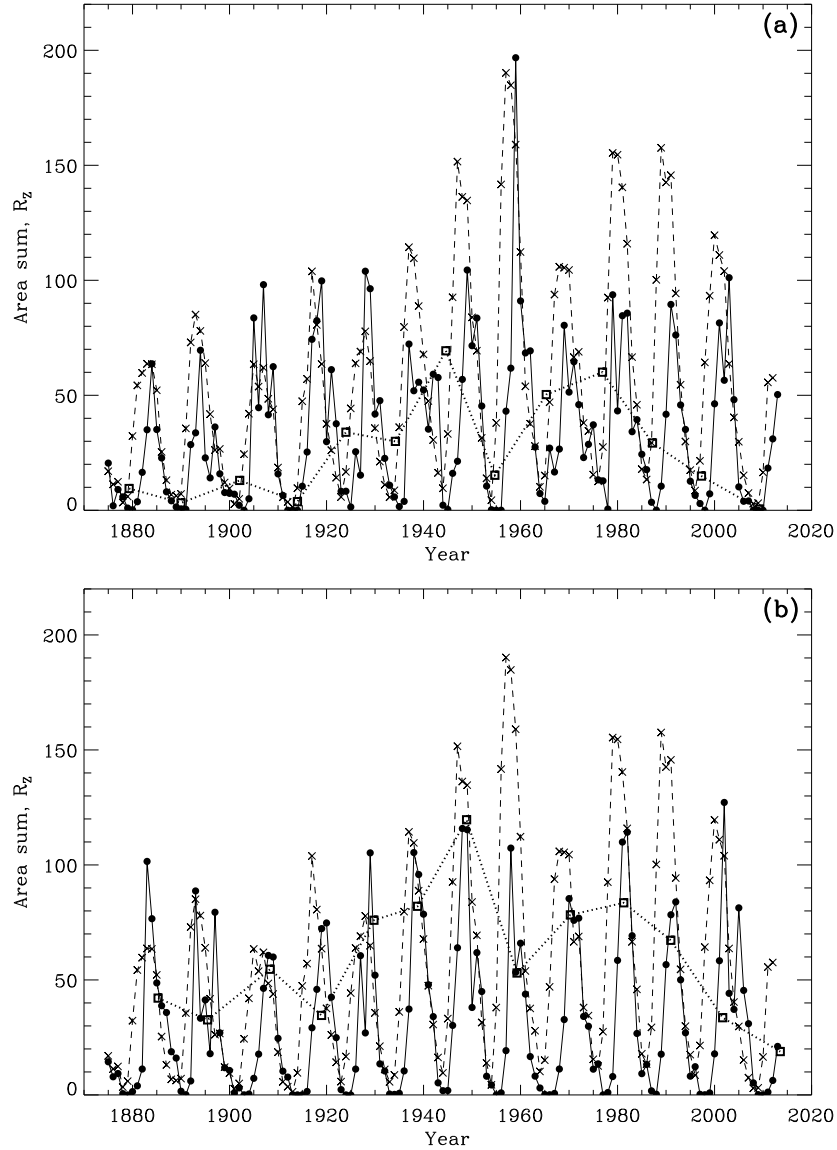


Figure 2: Variations in the annual sums (divided by 1000) of the areas of the sunspot groups (filled circle solid-curve),  $A_N(t)$  and  $A_S(t)$ , in  $0^\circ - 10^\circ$  latitude intervals of the northern hemisphere (upper panel) and the southern hemisphere (lower panel) during the period 1875–2013. The dotted-curves (with squares) represent the plots of  $A_N(T_m^*)$  (in upper panel) and  $A_S(T_M^*)$  (in lower panel) versus the middle epochs of  $T_m^*$  and  $T_M^*$ , respectively. In both the lower and upper panels the dashed-curve (with crosses) represents the annual variation of  $R_z$ .

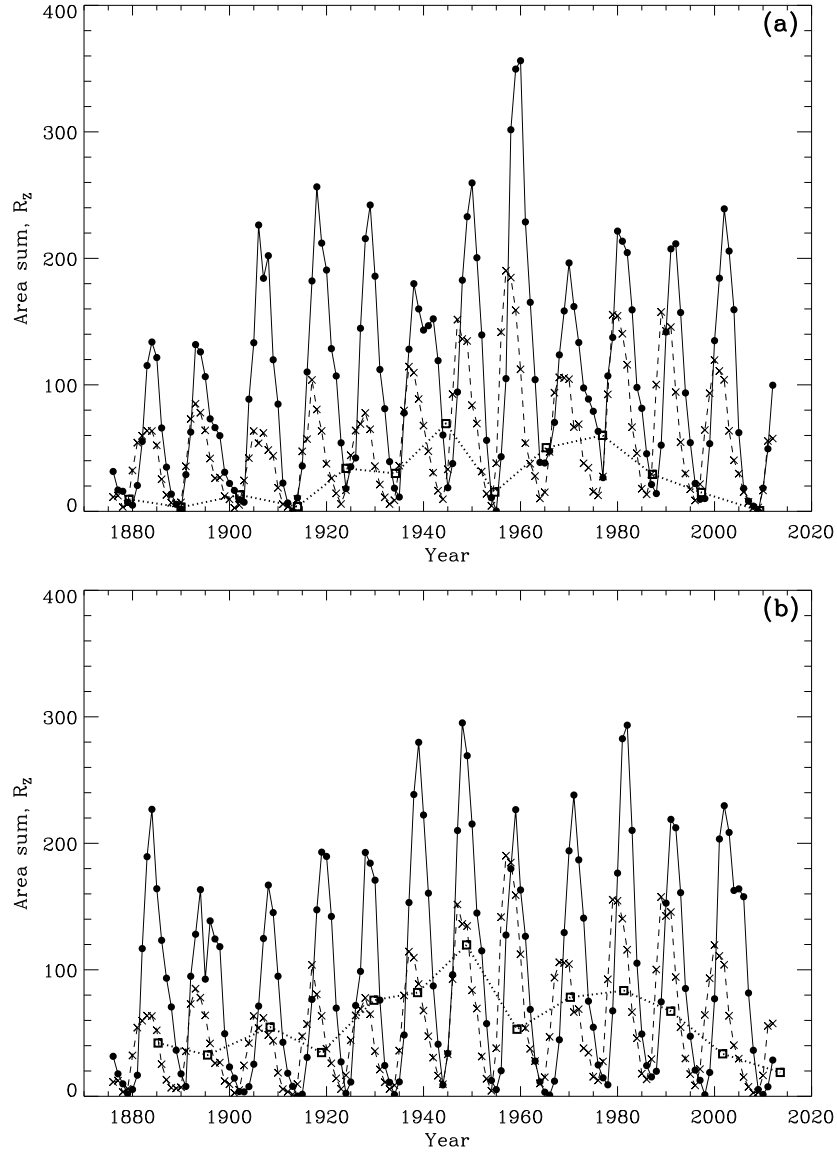


Figure 3: The same as Fig. 2 but the sums of the areas of the sunspot groups in the  $0^\circ - 10^\circ$  latitude intervals of the northern and southern hemispheres—determined by binning the sunspot group data during the period of 1875–2013 into the 3-year MTIs 1875–1877, 1876–1978, ..., 2010–2012, 2011–2013—versus the middle years 1976, 1977, ..., 2011, 2012 of the 3-year MTIs.

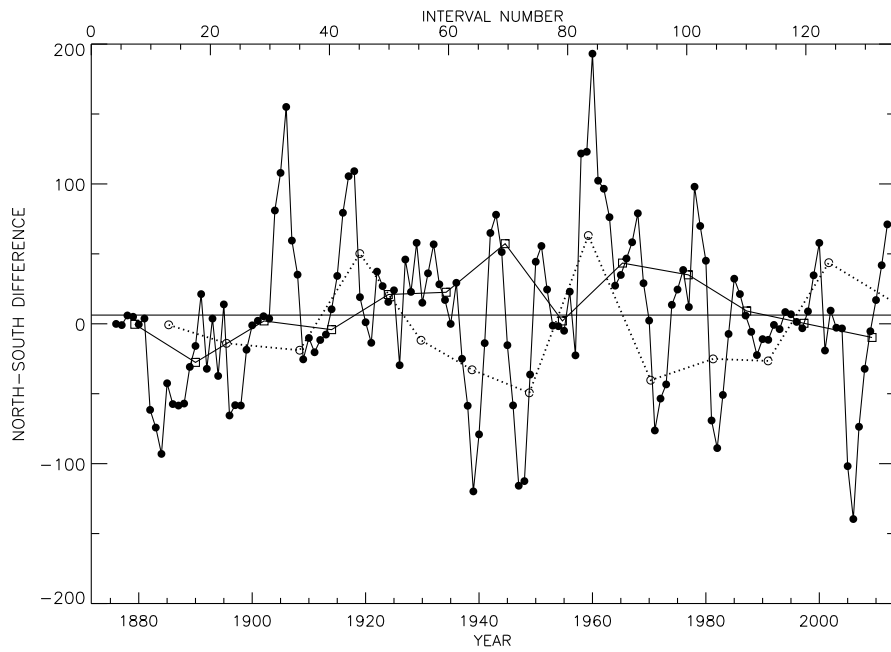


Figure 4: Plot of the differences between the sums of the areas of the sunspot groups in the  $0^\circ - 10^\circ$  latitude intervals of the northern and southern hemispheres versus middle years of the 3-year MTIs (closed circle-solid curve). The square-dashed and open circle-dotted curves represent the variations in the  $\delta A(T_m^*)$  and  $\delta A(T_M^*)$ , respectively.

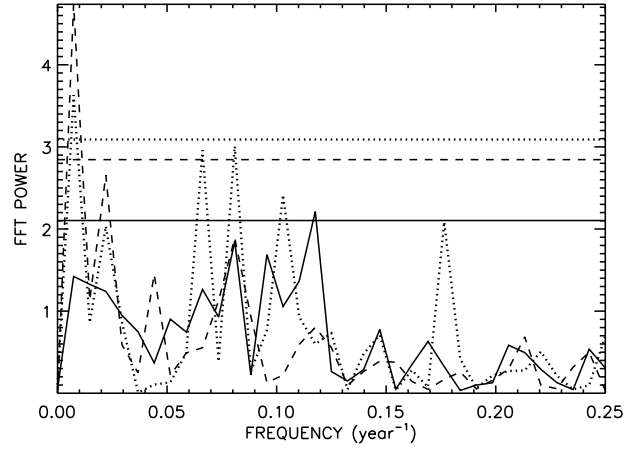


Figure 5: FFT power spectra of the north-south differences in the sums of the areas of the sunspot groups in  $0^\circ - 10^\circ$  (solid curve),  $10^\circ - 20^\circ$  (dotted curve), and  $20^\circ - 30^\circ$  (dashed curve), determined from 3-year MTIs during the period 1875–2013. The horizontal lines represent respective 99% confidence levels.

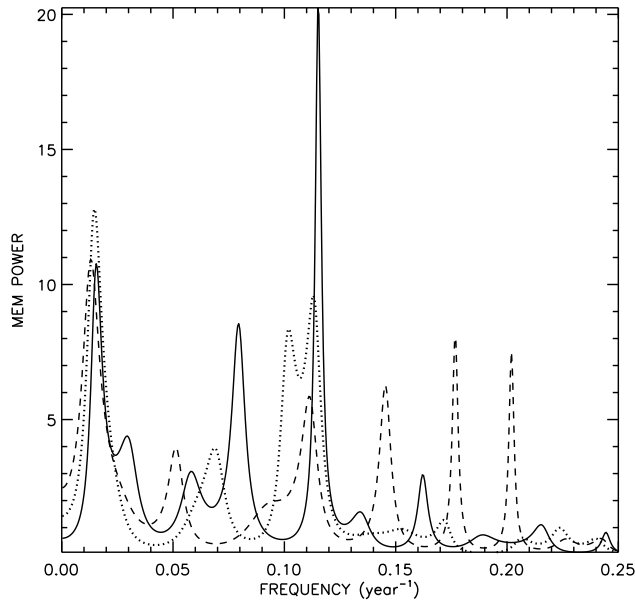


Figure 6: MEM power spectra of the north-south differences in the sums of the areas of the sunspot groups in  $0^\circ - 10^\circ$  (solid curve),  $10^\circ - 20^\circ$  (dotted curve), and  $20^\circ - 30^\circ$  (dashed curve), determined from 3-year MTIs during the period 1875–2013.

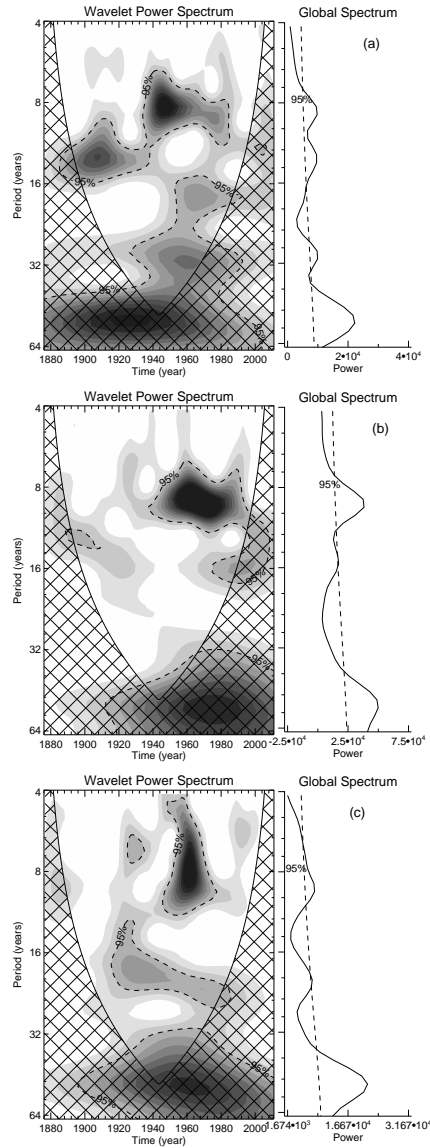


Figure 7: Wavelet power spectra and the global spectra of the north-south difference in the sums of the areas of the sunspot groups in (a)  $0^{\circ} - 10^{\circ}$ , (b)  $10^{\circ} - 20^{\circ}$ , and (c)  $20^{\circ} - 30^{\circ}$  latitude intervals, determined from the data in 3-year MTIs during the period 1875–2013. The wavelet spectra are normalised by the variances of the corresponding time series. The shadings are at the normalised variances of 1.0, 2.0, 3.0, 4.0, 5.0, 6.0, 7.0, 8.0 and 9.0. The dashed curves represent the 95% confidence levels, deduced by assuming a white noise process. The cross-hatched regions indicate the “cone of influence”, where edge effects become significant (Torrence and Compo 1998).

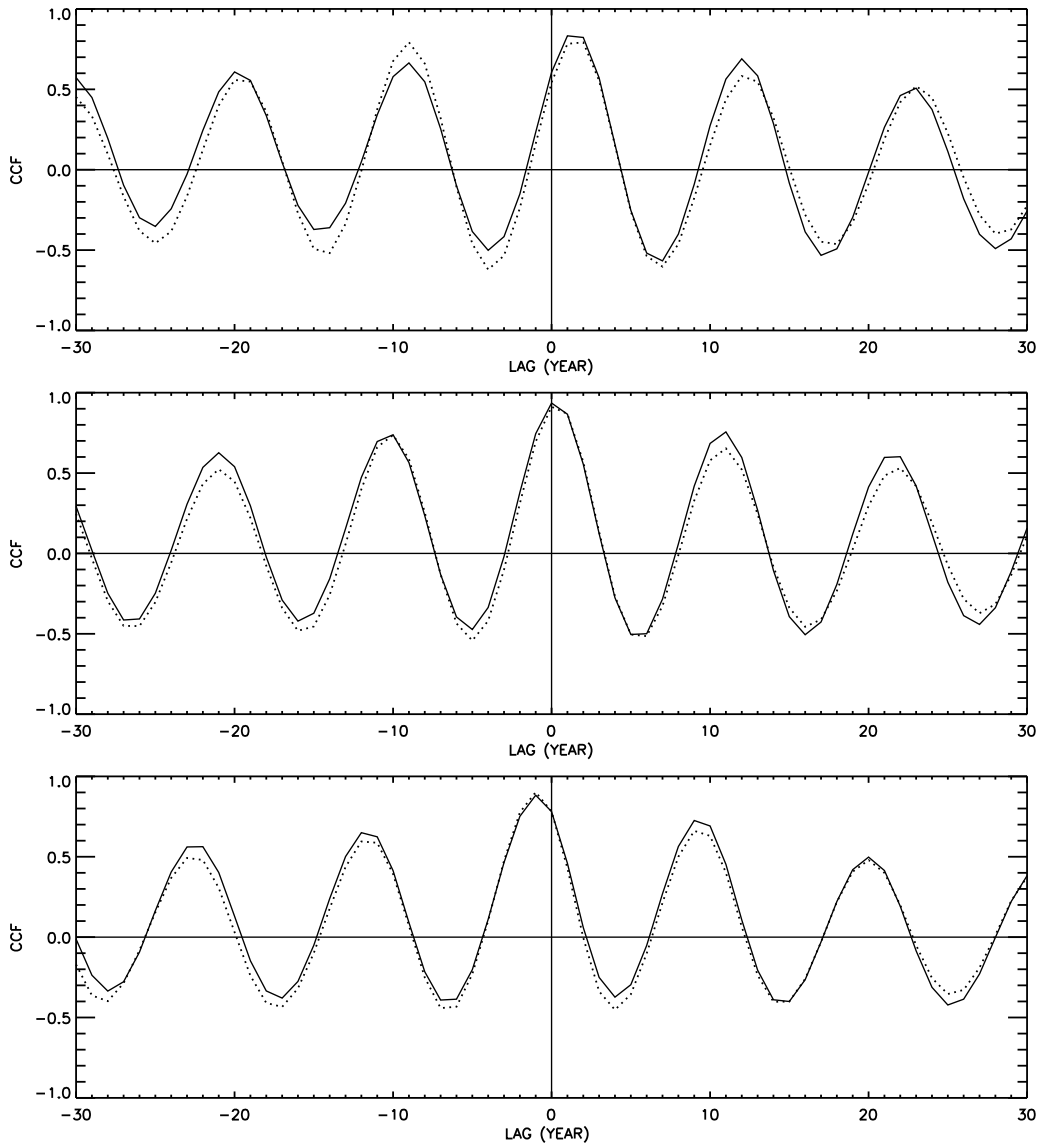


Figure 8: Plots of the cross-correlation coefficients  $CCF(R_Z, A_N)$  (solid curve) and  $CCF(R_Z, A_S)$  (dotted curve) versus Lag (year) in  $0^\circ - 10^\circ$  (top panel),  $10^\circ - 20^\circ$  (middle panel), and  $20^\circ - 30^\circ$  (bottom panel).



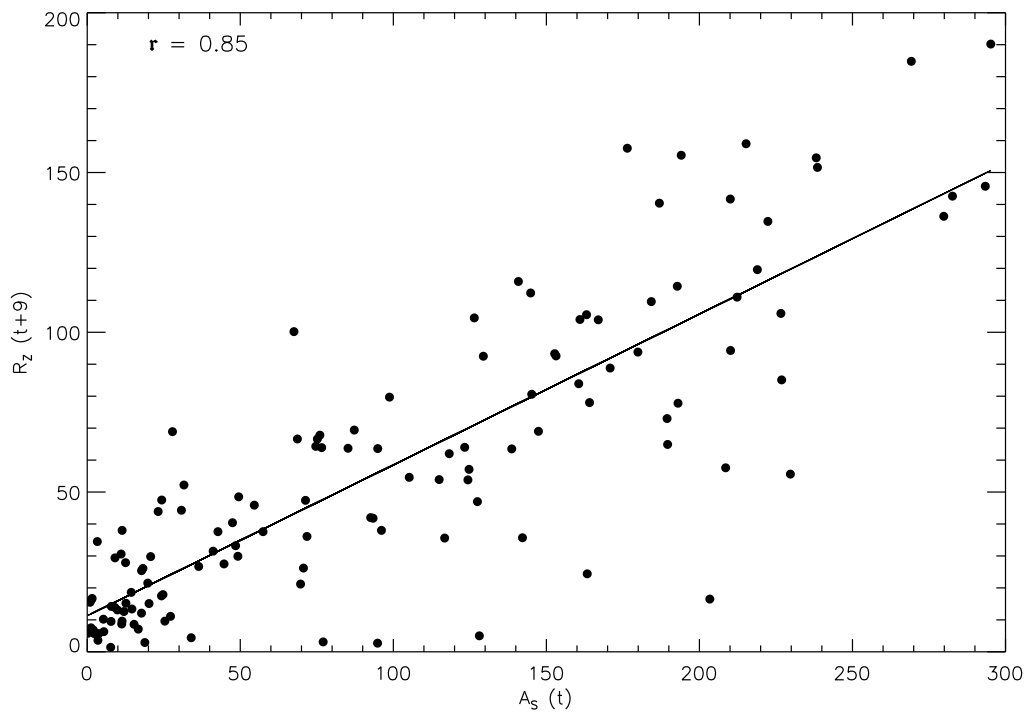


Figure 9: Scatter plot of  $A_S(t)$  of the sunspot groups in  $0^\circ - 10^\circ$  latitude interval of the southern hemisphere versus  $R_Z(t+9)$ , where  $t = 1976, 1977, \dots, 2011, 2012$  (in the case of  $A_S(t)$  they are the middle years of the 3-year MTIs 1875–1877, 1876–1978,  $\dots$ , 2010–2012, 2011–2013, respectively).

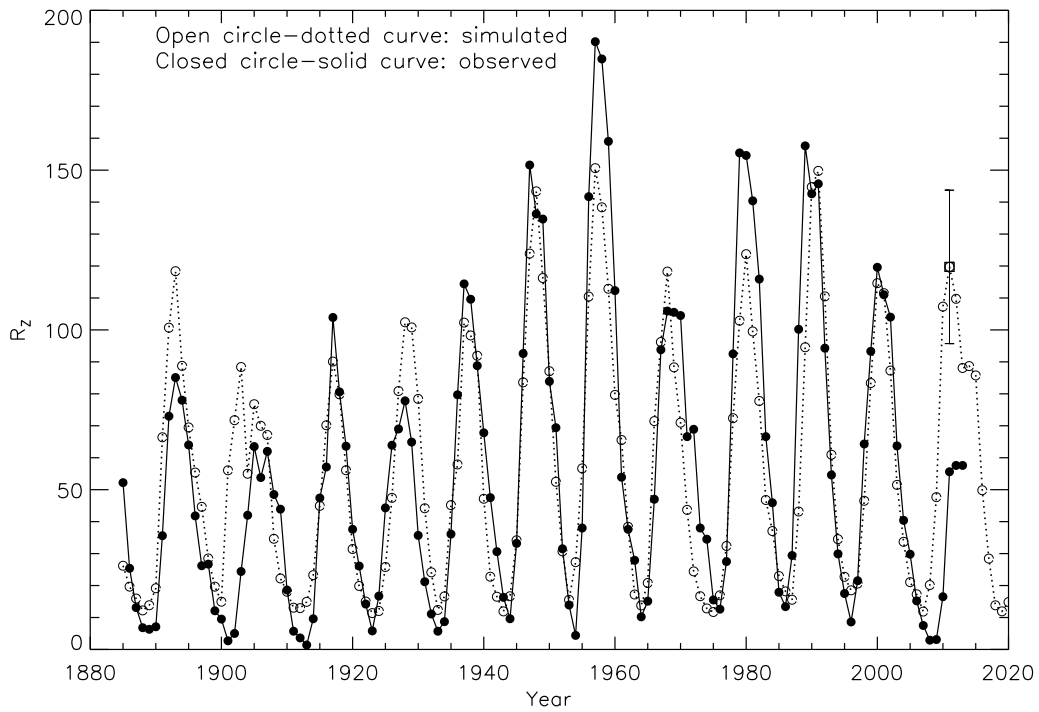


Figure 10: Plot of simulated (by using Eq. (4)) and observed values of  $R_Z$  versus time (year). The square at year 2011 represents the maximum of the simulated cycle 24 and the error bar represents the standard deviation of a simulate value.

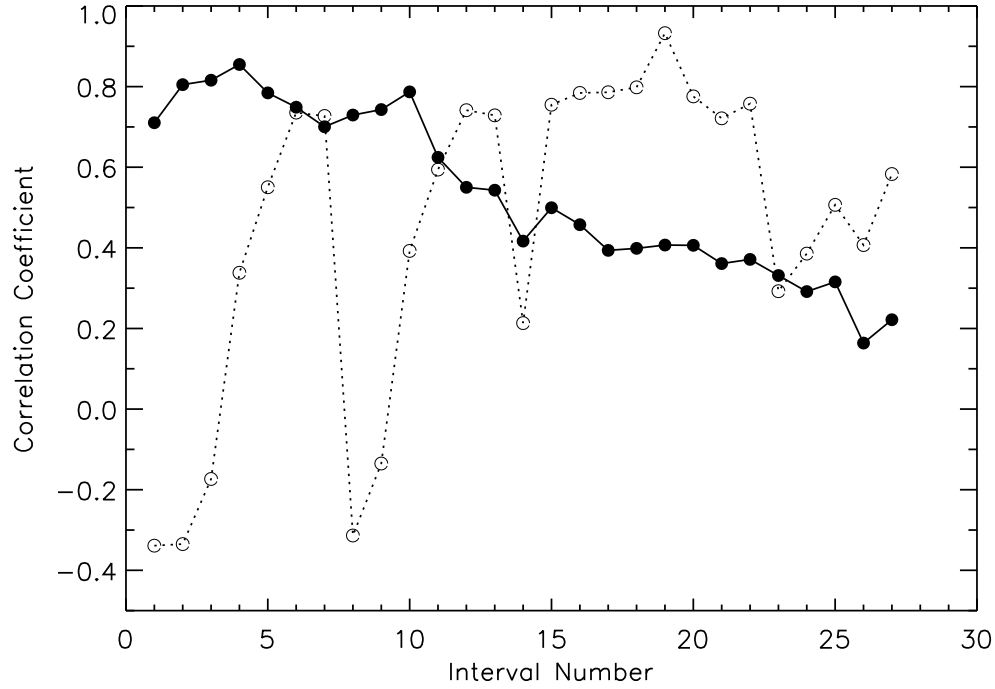


Figure 11: Changes in the correlations as the changes in  $T_m^*$  (solid curve) and in  $T_M^*$  (dotted curve). In this figure the end points of the time intervals (represented by interval numbers) are away from  $T_m$  and  $T_M$  as follows: Intervals 1, 2, 3, 4, ..., 7 are at (-2, -1), (-2, 0), (-2, 1), (-2, 2), ..., (-2, 5) years away, respectively; the end points of the intervals 8, 9, ..., 13 are at (-1, 0), (-1, 1), ..., (-1, 5) years away, respectively; similarly, the end points of the intervals 19, 20, ..., 22 are at (1, 2), (1, 3), ..., (1, 5) years away, respectively; and those of the intervals 26 and 27 are at (3, 4) and (3, 5) years away, respectively. In the intervals 4 and 19 the corresponding correlation coefficients have large values, 0.85 and 0.91, respectively. From  $T_m$  and  $T_M$  the end points of the intervals 4 and 19 are at (-2, 2) and (1, 2) years away, respectively, and obviously  $T_m^*$  and  $T_M^*$  are within these intervals, respectively.